PHYSICAL REVIEW VOLUME 187, NUMBER 2 10 NOVEMBER 1969

Electron Paramagnetic Resonance of Co-Doped PbWO$_4$[†]

MAO-CHIEH CHEN*
Research Laboratories, General Motors Corporation, Warren, Michigan 48090

AND

J. O. ARTMAN
Departments of Physics and Electrical Engineering, Carnegie-Mellon University, Pittsburgh, Pennsylvania 15213

(Received 13 May 1969)

The EPR of Co-doped PbWO$_4$ was observed at 9 GHz at temperatures below 16°K. Four sets of lines were seen, each characterized by an effective electronic spin S of $\frac{1}{2}$ and a nuclear spin I of $\frac{7}{2}$. The spectral parameters of one set in an appropriate coordinate system were as follows: g_i: 4.50, 6.20, and 2.07; and A_i (in GHz): 0.605, 0.970, and 0.248 ($i=x,y,z$). The Eulerian angles of this coordinate system with respect to the crystal axis system (caa) were: $\alpha=43.8°$, $\beta=28.0°$, and $\gamma=-65.3°$. The remaining three coordinate sets are obtained by increasing α in increments of 90°. Above 16°K, the spectra gradually became broad and weak, and finally at 20°K disappeared, clearly as a result of the onset of fast spin-lattice relaxation. Below 4.2°K, the relaxation times became so long that difficulty was encountered in recording the true line shape. We believe that Co enters this lattice in a 2+ state and probably substitutes at a W site. The ground state in this site of S_4 symmetry then would be $^4A_2$. From relaxation data, we estimate that the separation of the two sets of Kramers doublets is several tens of wave numbers. The EPR of Co-doped PbMoO$_4$ and PbWO$_4$ are essentially the same.

I. INTRODUCTION

MANY microwave investigations have been performed on paramagnetic ions in scheelite (CaWO$_4$) structures. The rare-earth ions especially, and also some $3d$ transition-metal ions, have been studied. Most investigations of the $3d$ transition-metal ions as dopants in the scheelites involved the S-state ions Fe^{3+} and Mn^{2+}.[1–7] Some results on other $3d$ ions have been reported: Cu^{2+}($3d^1$) in CaWO$_4$[8] and V^{4+}($3d^1$) in CaWO$_4$.[9] Besides these, Mo^{5+}($4d^1$),[10] W^{5+}($5d^1$),[11] and Nb($4d$ group)[12] have also been reported. Both the scheelite Ca and W sites possess tetrahedral-type S_4 symmetry. Considerations such as ionic size, chemical bonding, electrical neutrality, and crystal growth kinetics have been raised in discussions about site preference.[1,13] The extensively studied low-valence (3+ or 2+) dopant ions usually seem to prefer the divalent metal site. Nevertheless, there has been some controversy about Fe^{3+} and Nd^{3+} site occupancy in CaWO$_4$.[2]

Co normally exhibits the valences 2 and 3[14]; among these, tetrahedral Co^{3+} is rarely observed.[15] The monovalent and tetravalent states also are rarely observed. Divalent Co (configuration $3d^7$) has a ^4F ground state. A tetrahedral crystal field splits the sevenfold-degenerate level into a lower singlet $^4A_2$ and two higher triplets $^4T_2$ and $^4T_1$. The energy-level scheme, thus, is similar to that of Cr^{3+}-doped α-Al$_2$O$_3$ (ruby). The EPR of Co^{2+} in tetrahedral stereochemistry has been reported previously. The observations were made at liquid-He and N$_2$ temperatures. The cases studied include Co^{2+} in zincblende structure (fourfold coordination)[16–19]: CdS, CdTe, ZnSe, and ZnS; Co^{2+} in Cs$_3$CoCl$_5$ and Cs$_3$CoBr$_5$[20,21]; and Co^{2+} in fluorite structure (eightfold coordination)[19]: CaF$_2$ and CdF$_2$. In all of these cases, an effective spin of $\frac{3}{2}$ was assigned and $g_\parallel$ and $g_\perp$ values of about 2.3 were reported. In CdS, a D value value of 0.67 cm^{-1} was reported,[17] but another reference reported $D>2$ cm^{-1} for this system.[16] In Cs$_3$CoCl$_5$, a D value of -4.5 cm^{-1} was found.[21]

The Co hyperfine structure (nuclear spin $\frac{7}{2}$) has been observed by previous investigators (except in Cs$_3$CoCl$_5$,

---

[†] Supported in part by the U. S. Army Research Office, Durham.

[*] Based on a thesis submitted in partial fulfillment of the requirements for the degree of Doctor of Philosophy in Electrical Engineering from Carnegie-Mellon University.

[1] R. W. Kedzie, D. H. Lyons, and M. Kestigian, Phys. Rev. **138**, A918 (1965).

[2] R. W. Kedzie and M. Kestigian, Appl. Phys. Letters **3**, 86 (1963); **4**, 124 (1964).

[3] J. Kirton and R. C. Newman, Phys. Rev. Letters **15**, 244 (1965).

[4] R. W. Kedzie and D. H. Lyons, Phys. Rev. Letters **15**, 632 (1965).

[5] C. F. Hempstead and K. D. Bowers, Phys. Rev. **118**, 131 (1960).

[6] J. Bronstein and S. Maniv, Phys. Rev. **153**, 303 (1967).

[7] A. Kiel and W. B. Mims, Phys. Rev. **153**, 378 (1967).

[8] G. H. Azarbayejani, Bull. Am. Phys. Soc. **12**, 1044 (1967).

[9] N. Mahootian, C. Kikuchi, and W. Viehmann, J. Chem. Phys. **48**, 1097 (1968).

[10] G. H. Azarbayejani and A. L. Merlo, Phys. Rev. **137**, A489 (1965).

[11] G. H. Azarbayejani, Bull. Am. Phys. Soc. **10**, 1131 (1965).

[12] K. C. Chu, C. Kikuchi, and W. Viehmann, J. Chem. Phys. **46**, 386 (1967).

[13] K. Nassau and A. M. Broyer, J. Appl. Phys. **33**, 3064 (1962).

[14] A. F. Wells, *Structural Inorganic Chemistry* (The Clarendon Press, Oxford, 1962), 3rd ed, p. 911.

[15] C. J. Ballhausen, *Introduction to Ligand Field Theory* (McGraw-Hill Book Co., New York, 1962), p. 225.

[16] H. H. Woodbury and G. W. Ludwig, Bull. Am. Phys. Soc. **6**, 118 (1961).

[17] K. Morigaki, J. Phys. Soc. Japan **18**, 1558 (1963); **19**, 2064 (1964).

[18] F. S. Ham, G. W. Ludwig, G. D. Watkins, and H. H. Woodbury, Phys. Rev. Letters **5**, 468 (1960).

[19] T. P. P. Hall and W. Hayes, J. Chem. Phys. **32**, 1871 (1960).

[20] P. P. van Stapele, H. G. Beljers, P. F. Bongers, and H. Zijlstra, J. Chem. Phys. **44**, 3719 (1966).

[21] K. D. Bowers and J. Owen, Rept. Progr. Phys. **18**, 304 (1955).

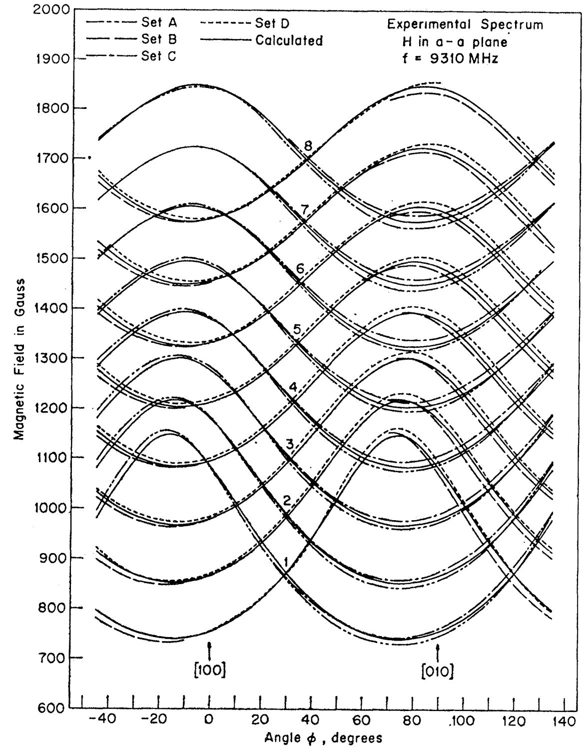

FIG. 1. Experimental and theoretically calculated spectra for the magnetic field in the *a*-*a* plane. The calculated spectrum is shown by solid lines located between each pair of experimental lines.

owing to large linewidths).[21] Hall and Hayes[19] resolved hyperfine structure in Co-doped CdF_2 at 20°K and in Co-doped CdTe at 4°K; the value of A, the hyperfine constant, in both was 23×10^{-4} cm^{-1}. Other hyperfine-constant tabulations include 23×10^{-4} cm^{-1} for CaF_2[19]; 17.5×10^{-4} cm^{-1} for ZnTe[18]; and a much smaller value of 1.8×10^{-4} cm^{-1} for ZnS.[18] In CdS, the hyperfine interaction was anisotropic[16,17]: $A_{\parallel}=(4.7\pm0.2)\times10^{-4}$ and $A_{\perp}=(10.5\pm0.6)\times10^{-4}$ cm^{-1}. We observed four groups of spectra in our samples. The presence of four groups of EPR spectra has been reported previously in transition-metal and rare-earth-ion-doped scheelites.[3–11,22,23] Two groups of spectra were reported[24] in $CaWO_4$ doped with Yb^{3+}. Controversy concerning site occupancy has arisen in these multiple-spectra cases.[2,23,24]

TABLE I. Crystallographic data for $PbWO_4$ and ionic radii of the ions of interest.

a	*c*	*x*	*y*	*z*
5.448 Å	12.016 Å	0.25±0.02	0.13±0.02	0.075±0.015

Distances (Å)		Angles	
W-O	1.780	O-W-O	119°10′ 104°51′
Pb-O	2.604	O-Pb-O	130°43′ 72°16′ 96°56′
	2.594		139°19′

Ionic radii (Å) (sixfold coordination)

O^{2-}	1.40	Co^{3+}	0.63
Pb^{2+}	1.20	W^{6+}	0.64
Co^{2+}	0.74		

II. CRYSTALLOGRAPHY

$PbWO_4$ has the scheelite structure, characterized by tetragonal symmetry with $a=b\neq c$ and $\alpha=\beta=\gamma=90°$. There are four molecules per unit cell. The space group is $I4_1/a(C_{4h}{}^6)$. Three special position parameters (x,y,z) are required for the specification of the oxygen positions. Crystallographic data for $PbWO_4$[25] as well as some ionic radii[26] of interest are listed in Table I. The variation of radius with coordination number may be represented as[27]

Coordination number	8	6	4
Radius	1.03	1.00	0.95.

The point symmetry at the Pb as well as W sites is S_4. Each Pb ion is surrounded by eight oxygen ions, each belonging to one of eight different WO_4 tetrahedra. The eight oxygen ions are divided into two groups of four each, forming two distorted interpenetrating tetrahedra; one set at a distance of 2.604 Å and the other at a distance of 2.594 Å from the Pb ion. (In a regular tetrahedron, all the O-Pb-O angles would be 109°28′.) The four oxygens about the W ion (at a distance of 1.780 Å) also form a slightly distorted tetrahedron.

III. EXPERIMENTAL TECHNIQUES AND RESULTS

A. Apparatus and Techniques

The EPR observations were made with a single klystron superheterodyne spectrometer operating at *X* band. The local oscillator signal necessary for superheterodyne action was obtained with a single side-band modulator.

A rectangular cavity with an unloaded *Q* of approximately 3000 and resonating in the TE_{102} mode at about 9400 MHz was used. The $PbWO_4$ (and $PbMoO_4$) crystals used in this investigation were grown by the Czochralski method and contained about 0.06% Co impurity. The samples used in the cavity were roughly circular in cross section and about 1 mm thick. One of the *a* axes was perpendicular to the flat circular face. By orienting the sample appropriately, the dc magnetic field could be applied in either the *c*-*a* or *a*-*a* plane. The

---

[22] V. Volterra, J. Bronstein, and M. Rockni, Appl. Phys. Letters 8, 212 (1966).

[23] C. G. B. Garrett and F. R. Merritt, Appl. Phys. Letters 4, 31 (1964).

[24] U. Ranon and V. Volterra, Phys. Rev. **134**, A1483 (1964).

[25] L. G. Sillén and A-L. Nylander, Arkiv Kemi Mineral. Geol. **17A**, No. 4 (1943).

[26] M. Clyde Day and Joel Selkin, *Theoretical Inorganic Chemistry* (Reinhold Publishing Co., Inc., New York, 1962).

[27] R. C. Evans, *An Introduction to Crystal Chemistry* (Cambridge University Press, Cambridge, England, 1966), 2nd ed., p. 86.

arrangement was such that all spectra were taken with the dc magnetic field perpendicular to the microwave magnetic field.

For reference purposes we used a small g-marker sample consisting of the colloidal Li particles formed in LiF by thermal neutron irradiation. The conduction electrons of these particles resonate at the free-electron g value 2.0023.

A simple resistance thermometer was used to measure the sample temperature. The carbon resistor was mounted on the outside of the cavity near the bottom and close to the sample crystal. A pumping scheme and a simple control circuit were set up for controlling the temperature below 20°K.

B. EPR Spectra

EPR spectra were observed primarily at 4.2°K and at temperatures between 10°–16°K in the vicinity of the hydrogen triple point. Figures 1 and 2 show the observed spectra with the external magnetic field sweeping in the a-a plane and c-a plane, respectively, of the crystal. All these spectra were observed in the temperature range 10–16°K. The presence of four groups of EPR spectra is evident. Each group consists of eight hfs components associated with the Co nuclear spin, $I=\frac{7}{2}$. The effective electron-spin value S is $\frac{1}{2}$. It is also apparent from the angular variation that an individual group does not possess axial symmetry. These four groups of EPR spectra coalesce into two groups when the magnetic field $\mathbf{H}$ is in the a-a plane and into one group when $\mathbf{H}$ is along the c axis.

As the temperature rose above 16°K, it was observed that the lines became broad and that the spectra gradually became weaker. The spectra disappeared at a temperature higher than, but obviously very close to, 20°K. This clearly is due to the onset of fast spin-lattice relaxation. The spectra were also observed at 4.2°K and showed no apparent decrease in intensity. However, as the temperature was reduced below 4°K, the line shapes dramatically changed from the ordinary first-derivative absorption patterns to anomalous shapes which looked like the second derivative of absorption. It is believed that these phenomena are associated with saturation and passage effects. This will be briefly discussed in Sec. III C.

In addition to those shown in Figs. 1 and 2, other resonance lines were also observed. Some of these are quite strong compared to the Co—by as much as one or two orders of magnitude. Some portions of the spectra shown in Figs. 1 and 2 were masked by these strong lines; the resonance line positions in such regions were interpolated and indicated by thinner lines. These extraneous lines did not exhibit hyperfine splittings. Most of these extra resonances were also observed at 77°K (when the Co spectra had disappeared) but all disappeared at room temperature. When the temperature was reduced to well below 4°K (where the Co line changed dramatically in appearance) these extra resonance lines exhibited no obvious change. This was true even at a temperature as low as 1.6°K. Clearly these extraneous lines are associated with another substituent.

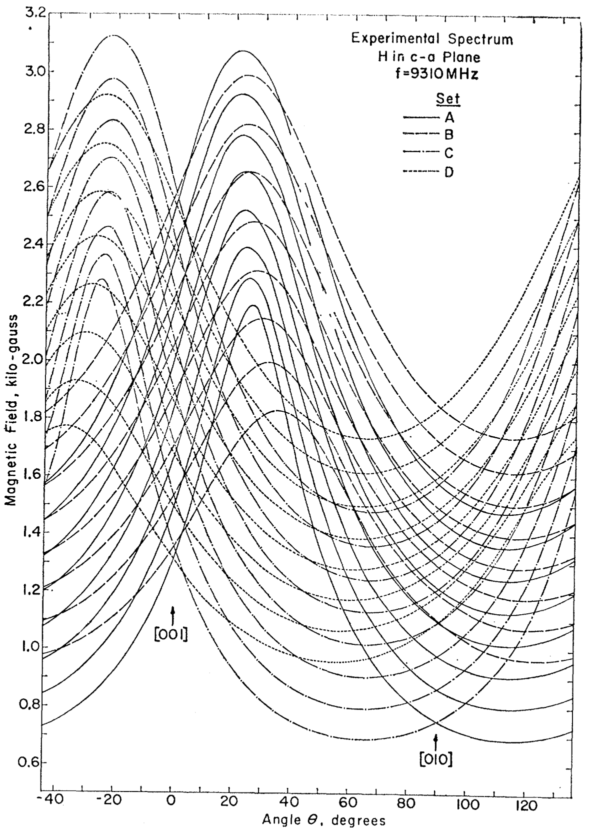

FIG. 2. Experimental spectrum for the magnetic field in the c-a plane. Portions of the spectrum that were masked by strong extraneous lines are interpolated and indicated by thinner lines.

C. Saturation Observations

All the EPR observations were performed with approximately 0.1 mW of microwave power incident upon the sample cavity. At these power levels, the Co line patterns appeared "normal" at 4.2°K. With this power level fixed, the absorption *increased* in intensity with increasing temperature to about 16°K. Above 16°K the lines became broad and weak and finally disappeared, obviously due to rapid spin-lattice relaxation. On the other hand, as the temperature was reduced below 4.2°K the normal line shape began to change strikingly while the intensity simultaneously *decreased*. An anomalous shape which looked like the second derivative of absorption, or the first derivation of dispersion, was finally clearly established near 3.5°K. Further temperature reduction (to as low as 1.5°K) did *not* cause any additional changes. Observations were also carried out at a power level of 10^{-7}W, the minimum power necessary to maintain our spectrometer properly frequency

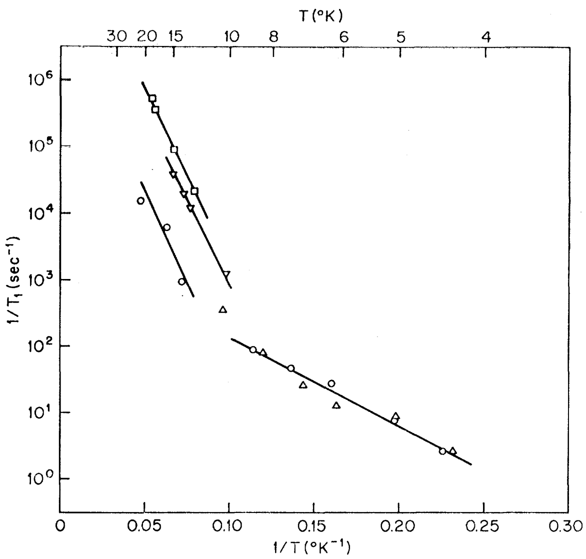

FIG. 3. Variation of spin-lattice relaxation rate $1/T_1$ with temperature T: $\log_{10}(1/T_1)$ versus $1/T$. The symbols ○, △, ▽ and □ represent data from different runs.

stabilized. Under such conditions the same effects were seen, although the temperature at which specific behavior was observed were shifted slightly downward.

It seems clear that these phenomena are associated with "passage effects"[28] (which are sensitive to temperature) in an inhomogeneously broadened system.[29] We must further assume that our bridge was not properly balanced—a small amount of dispersion has been mixed with the absorption. (This could have occurred inadvertently when balancing the bridge by use of the strong marker signal as a guide. Weger[28] pointed out that one may wish to unbalance a bridge slightly to reduce the slightly distorted appearance of *strong* resonances.) Above 4.2°K, passage effects and small bridge unbalances were not important. Below 4.2°K, we tend to saturate the absorption and see the weak dispersion. Passage effects are important here.

The importance of this saturation observation should be reemphasized here. The fact that the anomalous spectra did not change in intensity and still existed at the lowest temperatures available to us suggests that the Co spectra originate from transitions involving the *ground* state. The effects discussed here are due to passage and saturation phenomena and *not* to depopulation.

TABLE. II. Axis orientations and principal g-tensor values in Co-doped $PbWO_4$.

	x	y	z
g	4.50	6.20	2.07
θ^a	78.69°	64.75°	28.00°
$\phi_1{}^b$	335.90°	71.32°	43.80°
ϕ_2	65.90°	161.32°	133.80°
ϕ_3	155.90°	251.32°	223.80°
ϕ_4	245.90°	341.32°	313.80°

[a] θ is the angle between each tensor principal axis and the c-axis of the crystal.

[b] ϕ is the angle between the projection of the tensor principal axis on the a-a plane and an a axis. Right-handed rotation is taken as positive; ϕ_1 to ϕ_4 refer to the four sets of principal-axis directions.

D. Relaxation Time Measurements

We attempted to estimate the spin-lattice (i.e., spin-phonon) relaxation time T_1 by the cw method. The particular sample used in these relaxation observations was a Co-doped $PbMoO_4$ sample charged compensated with Na. Although a spin-Hamiltonian fit was not made for this crystal, the positions of the Co resonances appeared virtually identical to those in the uncompensated $PbWO_4$ sample. Also, the line shapes (and the temperature behavior) of this charge-compensated sample were the same as that of the uncompensated sample used earlier for the spectra observations.

The spin-lattice relaxation time T_1 was evaluated between 4.2 and 20°K. The curves are plotted in Figs. 3 and 4. Data points from different runs are indicated by different symbols: ○ △ ▽ □. Although the accuracy of the numerical value of T_1 found may be questionable, the general trend of T_1 versus temperature should be reliable. It is clear that the high- and low-temperature slopes of the plots differ, indicating the presence of at least two relaxation mechanisms.

IV. THEORY AND DISCUSSION

A. Phenomenological Spin Hamiltonian

Careful examination of the angular variation of the spectra suggest the following g-tensor model: each of the four spectral groups is characterized by a g tensor having three unequal principal values (oriented along directions none of which is a crystal axis direction) and

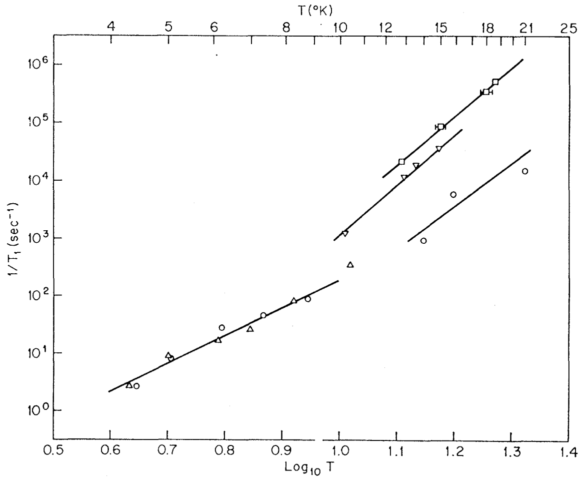

FIG. 4. Variation of spin-lattice relaxation rate $1/T_1$ with temperature T: $\log_{10}(1/T_1)$ versus $\log_{10}T$. The symbols ○, △, ▽ and □ represent data from different runs.

---

[28] M. Weger, Bell System Tech. J. **39**, 1013 (1960).

[29] A. M. Portis, Phys. Rev. **91**, 1071 (1953).

related to the remaining three groups by rotations of 90°, 180°, and 270° about the c axis.

In each g-tensor principal-axis system, the spectrum was fit to a spin Hamiltonian of the form

$$\mathcal{H}=\beta(g_zH_zS_z+g_xH_xS_x+g_yH_yS_y)+A_zI_zS_z+A_xI_xS_x+A_yI_yS_y\,,$$

with $S=\frac{1}{2}$ and $I=\frac{7}{2}$, and[30]

$$g_x=4.50\,,\quad A_x=0.605\text{ GHz}=201.7\times10^{-4}\text{ cm}^{-1}\,,$$
$$g_y=6.20\,,\quad A_y=0.970\text{ GHz}=323.3\times10^{-4}\text{ cm}^{-1}\,,$$
$$g_z=2.07\,,\quad A_z=0.248\text{ GHz}=\ 82.7\times10^{-4}\text{ cm}^{-1}\,.$$

The three Eulerian angles α, β, and γ characterizing the principal coordinate system of one such group with respect to the crystal axis (caa) system are, respectively, 43.8°, 28.0°, and −65.3°. The axis orientations derived from these data and the principal values of the g tensor are summarized in Table II. Table III lists the direction cosines of the g-tensor principal axes with respect to the crystal axes. Figure 5 depicts the orientation of one set of the g-tensor principal axes with respect to the crystal axes. The remaining three sets are not shown, but can be readily obtained by rotations of 90°, 180°, and 270° about the crystal c axis. To clarify the symmetry relations, a view of the four g-tensor sets along the crystal c axis is shown in Fig. 6. Only the axis with the principal value of 2.07 is shown here (in projection).

Because of the symmetry, resonance sets A and C, and separately B and D, are indistinguishable when **H** is applied in the a-a plane. Furthermore, the resulting two spectral sets are related by a 90° shift on the angular coordinate axis. In general, the four spectral sets are nonequivalent in the c-a plane. However, the four sets must coalesce into one when **H** is directed along c. Parts of the experimental c-a plane spectrum for groups A, B and C, D at two different orientations are shown in Figs. 7 and 8, respectively. From symmetry, the group-C spectrum can be generated from the group-A spectrum by reflection through the c-axis line. The same relation exists between groups B and D. Similarly another symmetry axis exists in the c-a plane: the a axis, for example [010], which is marked as 90° in Figs. 2 and 8. The group-A spectrum can also be generated from the group-C spectrum by reflection through the a-axis line. This same relation also holds between groups B and D. For this reason we plot only the C and D spectra in Fig. 8. Similarly, we show only the A and B spectra in Fig. 7.

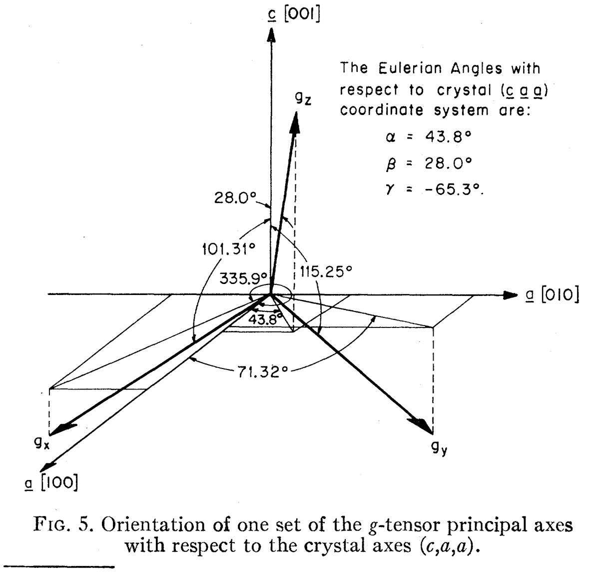

FIG. 5. Orientation of one set of the g-tensor principal axes with respect to the crystal axes (c,a,a).

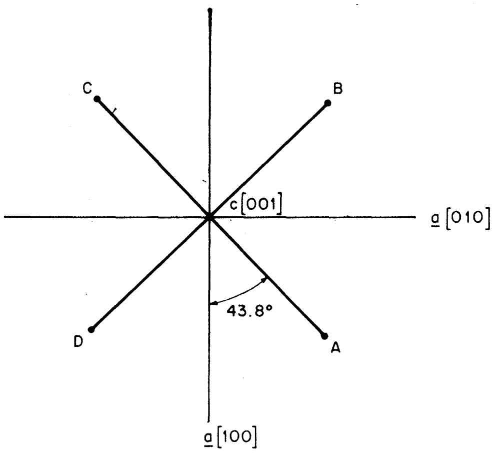

FIG. 6. A view along the c axis of the four g-tensor sets. Only the axis with the principal value of 2.07 is shown here (in projection).

Theoretically calculated results were plotted in Fig. 1 and also in Figs. 7 and 8 for comparison with the experimental observations. In general, the calculated curves correspond closely to the experimental, although the match in some parts of Fig. 7 is not very good. As shown in Fig. 1, the experimental a-a plane spectrum is split into two in some angular regions with the theoretical (unsplit) lines situated within the experimental split ones. We have attributed these small splittings to small sample misorientations of not more than 1° or 2°. Similarly, the two groups of lines observed when the magnetic field is along the c axis (Figs. 2 and 7) can also be attributed to small misorientations. Although four groups of lines would be expected, we presume that we

TABLE III. Direction cosines of the g-tensor principal axes with respect to the crystal axes ($a=b\neq c$).

g_i	cos(i,a)	cos(i,b)	cos(i,c)
g_x	0.8952	−0.4004	−0.1961
g_y	0.2897	0.8570	−0.4266
g_z	0.3387	0.3272	0.8829

---

[30] The x and y of the entries in these listings correspond, respectively, to the y and x of the expressions in Sec. IV C.

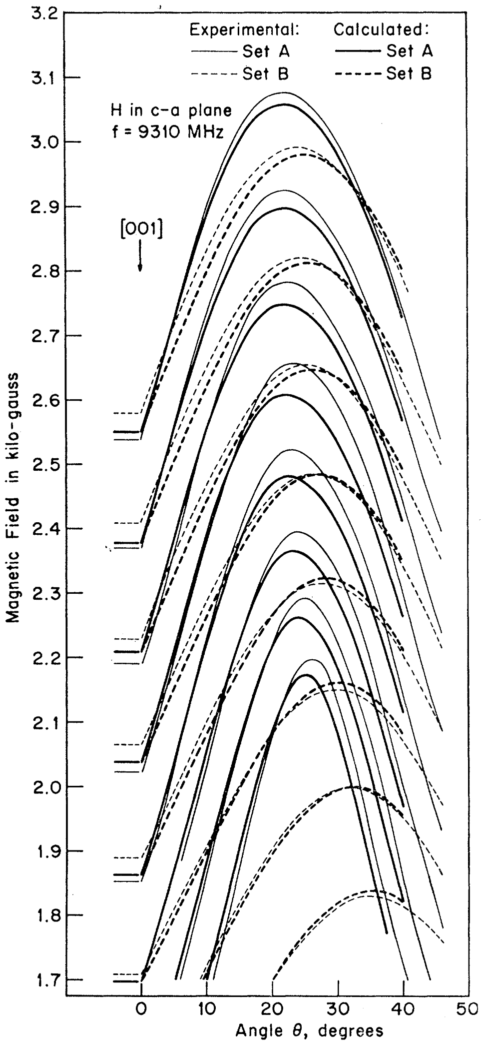

FIG. 7. Comparison of the experimental and theoretically calculated spectra (sets A and B) for the magnetic field in the *c*-*a* plane at an orientation near $\theta=20°$.

were unable to resolve additional splittings in the components of the two observed groups.

B. Oxidation State of Co

Before discussing all reasonably conceivable oxidation states of Co (1+, 2+, 3+, and 4+) it is worthwhile here to recapitulate relevant experimental observations. The resonance transition occurred in a ground doublet state; it could not be observed at temperatures above 20°K, and the spectroscopic g factor was highly anisotropic.

Co^{1+} and Co^{3+} are in the $3d^8$ and $3d^6$ configurations, respectively. We expect the ground states arising from the splitting of these even-electron configurations by low-order crystal fields and Jahn-Teller effects to be *singlets*. This obviously disagrees with our experimental evidence. Analyses pertinent to high-spin Co^{3+} in a tetrahedral environment have been given by Low and Weger,[31] and Sharma and Artman.[32] Weakliem[33] and Kotani[34] have discussed the low-spin case. Siegert[35] analyzed the "mirror" configuration: V^{3+}($3d^2$) in an octahedral site. The separation between the ground singlet and the first excited doublet in V^{3+}-doped α-Al$_2$O$_3$ (octahedral site) was estimated to be 7 cm^{-1}.[36–38] Since the spin-orbit coupling constant of Co^{3+} is greater than that of V^{3+},[39] it is unlikely that the zero-field splitting for Co^{3+} in a tetrahedral site would be less than this. This of course contradicts the experimental evidence. Since the ground state of Co^{1+} in a tetrahedral field is the same as that of low-spin Co^{3+}, the arguments above are applicable. In any case, Co^{1+} is a relatively unlikely Co valence state.

Co^{4+} and Co^{2+} are in the $3d^5$ and $3d^7$ configurations, respectively. Since these are odd-electron configurations, we expect the ground states to be Kramers doublets. This *is* in accord with our evidence. More explicitly, the ground state for the high-spin Co^{4+}($3d^5$) state is an orbital singlet ^{6}S. The combined action of spin-orbit coupling and axial or rhombic crystal field components would split the ground configuration into three closely lying Kramers doublets.[40,41] S-state ions have important properties from the resonance point of view: a g-value very close to the free-electron value of 2.0023, an initial-level splitting of the order of a few tenths of a wave number, and a long spin-lattice relaxation time. Since our experimental observations do not correspond to any of the above, it is therefore very unlikely that we have high-spin Co^{4+}.

The low-spin Co^{4+} case must also be considered. In the case of very strong crystal fields, or possibly from covalent bonding,[21,42] the ground state of a d^5 complex would be $^2T_2$. In such a case, the effects of spin-orbit coupling and lower-symmetry crystal fields would leave the ground state with a twofold spin degeneracy,[21] i.e., $S=\frac{1}{2}$. Low-lying levels will exist within a few hundred degrees ($T=h\nu/k$) of the ground state. At high temperatures, rapid spin-lattice relaxation will broaden the lines; thus, paramagnetic resonance would only be

---

[31] W. Low and M. Weger, Phys. Rev. **118**, 1119 (1960).

[32] K. K. Sharma and J. O. Artman (unpublished).

[33] H. A. Weakliem, J. Chem. Phys. **36**, 2117 (1962).

[34] M. Kotani, J. Phys. Soc. Japan **4**, 293 (1949).

[35] A. Siegert, Physica **4**, 138 (1937).

[36] G. M. Zverev and A. M. Prokhorov, Zh. Eksperim. i Teor. Fiz. **38**, 449 (1960) [English transl.: Soviet Phys.—JETP **11**, 330 (1960)].

[37] S. Foner and W. Low, Phys. Rev. **120**, 1585 (1960).

[38] M. H. L. Pryce and W. A. Runciman, Discussions Faraday Soc. **26**, 34 (1958).

[39] D. S. McClure, in *Solid State Physics*, edited by F. Seitz and D. Turnbull (Academic Press Inc., New York, 1959), Vol. 9, p. 428.

[40] J. H. van Vleck and W. G. Penney, Phil. Mag. **17**, 961 (1934).

[41] A. Abragam and M. H. L. Pryce, Proc. Roy. Soc. (London) **A205**, 135 (1951).

[42] B. Bleaney and M. C. M. O'Brien, Proc. Phys. Soc. (London) **B69**, 1216 (1956).

observed at low temperatures. Very anisotropic g values have also been reported.[2,43]

Now consider the case when the Co^{4+} ion substitutes at the W site. If we extrapolate from the Co^{2+} and Co^{3+} ionic radii values listed earlier and examine the tabulated W-O distance, it seems reasonably clear that covalent bonding would be expected. The analysis immediately above would be applicable. We then expect a magnetic moment value ($\mu = g[S(S+1)]^{1/2}$) of 1.732 μ_B. This μ value of course has to be corrected for ortital contributions introduced through spin-orbit coupling. In practice, magnetic moments of more than 1.732, but in no case exceeding 2.6, have been found for a number of ions in the d^5 configuration with a $^2T_2$ ground term.[44] For Mn^{2+} and Fe^{3+} in cyanide compounds, for example, values between 1.97 and 2.50 were reported.[34] This is inconsistent with our result; the estimated magnetic moment, using the g values of our experimental observation, is about 4.

Suppose, on the other hand, that the Co^{4+} ion is located at the Pb site. From our atomic radii and lattice distance tabulations we expect ionic bonding. Extrapolating from the Co^{2+} and Co^{3+} optical observations in the garnets,[45] we estimate the crystal-field strength Dq for the eight-coordination site to be 2000 cm^{-1}. Extrapolating from tabulated information,[46] we estimate the Racah parameter B for Co^{4+} to be 1200 cm^{-1}. Now according to the Tanabe-Sugano diagram for d^5 ions, the discontinuity corresponding to the change of ground term takes place at the Dq/B value of 2.8. Hence, a Dq value exceeding 3360 cm^{-1} would be required for stabilization of the low-spin configuration. However, we have estimated Dq to be no more than 2000 cm^{-1}; therefore, the spin-paired configuration is unlikely.

Now let us consider $Co^{2+}(3d^7)$. In a tetrahedral crystal field, the ^4F ground state splits into a lower-orbital singlet $^4A_2$ and two excited-orbital triplets $^4T_2$ and $^4T_1$. Spin-orbit coupling will not lift the fourfold spin degeneracy in first order. However, in the presence of lower-symmetry crystal-field components, the $^4A_2$ state will split into two Kramers doublets. The fact that the observed spectrum is described by an effective spin of $\frac{1}{2}$ indicates, if this case is applicable, that the zero-field splitting is too large to be spanned by our X-band frequency quantum. Although the microwave spin-lattice relaxation time seems to be unusually short in contrast to that usually, but not invariably, associated with an A_2 state, an inspection of the optical spectrum leads to the conclusion that Co is in the 2+ valence state and probably substitutes at a W site.

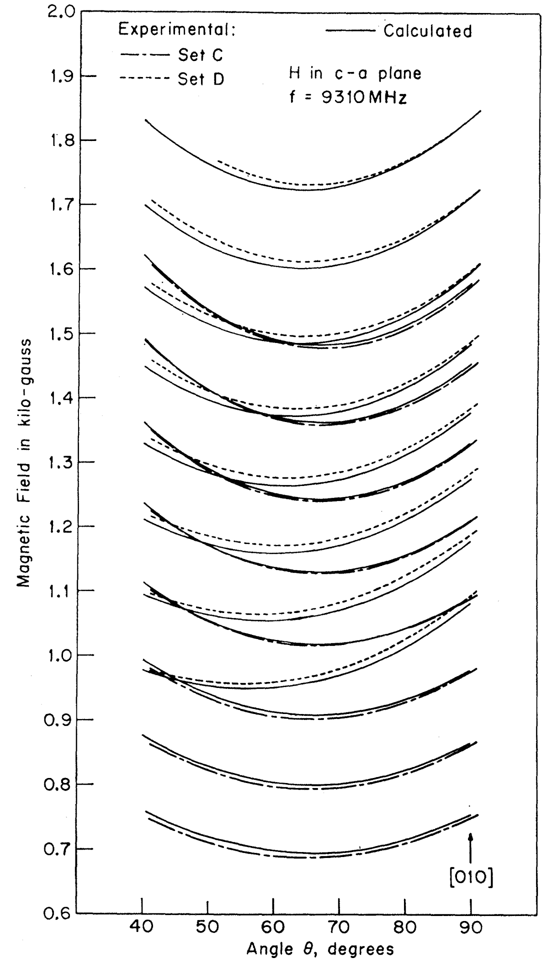

FIG. 8. Comparison of the experimental and theoretically calculated spectra (sets C and D) for the magnetic field in the c-a plane at an orientation near $\theta = 65°$.

The optical-absorption spectra of Co-doped $PbWO_4$ and $PbMoO_4$ have been examined briefly.[32] They were similar in appearance. The spectrum of the $PbMoO_4$ sample was analyzed in some detail; we presume that the findings in this system apply to both crystals. At room temperature in c polarization a few bands were seen in the visible region: one absorption maximum at 16130 cm^{-1} and three other weaker bumps at 15150, 18180, and 19230 cm^{-1}; in a polarization the latter two bumps apparently became too weak to be observed; the others, although also weaker, remained at the same wavelength positions. No other absorption besides this was observed. Wood and Remeika[45] have made extensive optical observations on Co-doped garnets. Their research is extremely pertinent since, in addition to octahedral sites, two types of tetrahedral sites exist in the garnets; one has four nearest-neighbor oxygens (called "tetrahedral" by Wood and Remeika), the other has eight nearest-neighbor oxygens (called" dodecahedral" by Wood and Remeika). The stereochemistries of

---

[43] J. M. Baker, B. Bleaney, and K. D. Bowers, Proc. Phys. Soc. (London) **B69**, 1205 (1956).

[44] B. N. Figgis, *Introduction to Ligand Fields* (Interscience Publishers, Inc., New York, 1966), p. 272.

[45] D. L. Wood and J. P. Remeika, J. Chem. Phys. **46**, 3595 (1967).

[46] B. N. Figgis, *Introduction to Ligand Fields* (Interscience Publishers, Inc., New York, 1966), p. 52.

these sites are thus similar to those of the W and Pb sites, respectively, in $PbMoO_4$. The tetrahedral cation-anion distance is 1.761 Å in yttrium gallium garnet YGG and 1.894 Å in yttrium aluminum garnet YAG[47]; the W-O distance in $PbWO_4$ is 1.780 Å and the Mo-O distance in $PbMoO_4$ is 1.781 Å. The garnet dodecahedral-site cation-anion distance is about 2.4 Å; the Pb-O distance is about 2.6 Å in $PbWO_4$ and $PbMoO_4$. The absorption spectrum of tetrahedral Co^{2+} in YAG garnet at 77°K clearly shows all the three spin-allowed transitions; i.e., a strong and sharp ${}^4A_2 \rightarrow {}^4T_1(P)$ band at 0.6 μ, a broad and not so strong ${}^4A_2 \rightarrow {}^4T_1(F)$ band around 1.2 μ, and a very sharp and weak ${}^4A_2 \rightarrow {}^4T_2(F)$ band at 2.1 μ. However, at 300°K the ${}^4A_2 \rightarrow {}^4T_2(F)$ band is almost invisible, the broad ${}^4A_2 \rightarrow {}^4T_1(F)$ band widens still further and thus becomes weaker making it difficult to discern its structure, while the ${}^4A_2 \rightarrow {}^4T_1(P)$ band still remains quite strong. In view of these results, we interpret the optical spectra of Co-doped $PbMoO_4$ and $PbWO_4$ as follows: The band observed at 16130 cm^{-1} corresponds, we believe, to the ${}^4A_2 \rightarrow {}^4T_1(P)$ of Co^{2+} in the garnet tetrahedral site, while both the ${}^4A_2 \rightarrow {}^4T_1(F)$ and ${}^4A_2 \rightarrow {}^4T_2(F)$ bands are just too weak and broad to be seen at room temperature. Following the Wood-Remeika analysis, we presume that the remaining weaker bumps near the supposed ${}^4A_2 \rightarrow {}^4T_1(P)$ absorption in the optical spectra of Co^{2+} in $PbMoO_4$ and $PbWO_4$ are due to the spin-forbidden transitions from the ground state to components of the ${}^2G$ doublet ${}^4A_2 \rightarrow {}^2E({}^2G)$ and ${}^4A_2 \rightarrow {}^2T_1({}^2G)$. Similar spectra were seen by Pelletier-Allard[48] in her optical investigations of Co^{2+} in Cs_3CoCl_5. The situation in which ${}^4T_1({}^4P)$, ${}^2T_1({}^2G)$, and ${}^2E({}^2G)$ are about the same energetically will occur, according to the Tanabe-Sugano diagram, when Dq/B has approximately the value 0.4. Taking $B = 1120$ cm^{-1} for Co^{2+},[46] we find Dq to be 448 cm^{-1}. This is in close agreement with the predictions and observations of Wood and Remeika in the case of tetrahedral Co^{2+} in garnets.[45] The fact that in our case the c- and a-polarized absorptions occur at the same wavelengths is probably due to a complicated averaging associated with the presence of four nonequivalent sites, none of whose axes of symmetry bear any simple relation to crystal geometry.

We believe that we can rule out Co^{2+} at the Pb site. Wood and Remeika[45] had predicted that the optical transitions of Co^{2+} in the dodecahedral garnet sites should occur at twice the frequency as that of Co^{2+} in the tetrahedral garnet sites. On this basis, they attributed an absorption (found experimentally at a frequency somewhat lower than predicted) to dodecahedral Co^{2+}. Weakliem had indicated[33] that the variation of the crystal-field Dq value is not sensitive to variation of the cation-anion distance. The assumption of Pb site (eight-coordination) substitution will therefore correspond to a Dq value much larger (approximately twice) than that of a W site (four-coordination) substitution but somewhat reduced[49] because of the longer bond distance. In view of these considerations and the previous arguments, we believe that Co enters the lattice in a 2+ state and probably substitutes at the tetrahedral four-coordinated W site.

C. Anisotropic g Tensor

The highly anisotropic g tensor indicates that the crystal field must undergo a rather substantial distortion from cubic symmetry. We have argued that we have Co^{2+} in a ${}^4A_2$ ground state; however, our observed effective spin value was $\frac{1}{2}$. We therefore propose a scheme which presumes a large zero-field splitting compared to the Zeeman term. First, we operate with a spin-$\frac{3}{2}$ Hamiltonian (hyperfine terms not shown)

$$\mathcal{H} = D[S_z^2 - \tfrac{1}{3}S(S+1)] + E(S_x^2 - S_y^2)$$

upon the orbital singlet ground state ${}^4A_2$. After diagonalization of the interaction matrix, we will account for Zeeman splittings by perturbation methods. The results of the evaluation of the eigenstates and g factors of the ground Kramers doublet are

$$\psi_1 = C_1|\tfrac{3}{2}\rangle + C_2|-\tfrac{1}{2}\rangle,$$
$$\psi_2 = C_1|-\tfrac{3}{2}\rangle + C_2|\tfrac{1}{2}\rangle,$$
$$g_z' = g_z(C_2^2 - 2C_1^2),$$
$$g_x' = g_x(C_2^2 + \sqrt{3}C_1C_2),$$
$$g_y' = 2g_y(C_2^2 - \sqrt{3}C_1C_2),$$

where

$$C_1 = \left(\frac{3E^2}{2D^2 + 6E^2 + 2D(D^2 + 3E^2)^{1/2}}\right)^{1/2},$$

$$C_2 = \left(\frac{2D^2 + 3E^2 + 2D(D^2 + 3E^2)^{1/2}}{2D^2 + 6E^2 + 2D(D^2 + 3E^2)^{1/2}}\right)^{1/2},$$

and g_z', g_x', and g_y' are the three "apparent" g-tensor components; g_z, g_x, and g_y are the three "intrinsic" principal g-tensor values appropriate before the mixing of the spin states by the D and E terms.

We attempted to correlate these calculated expressions with the experimental observations. The experimetal values are $g_z' = 2.07$, $g_x' = 6.20$, and $g_y' = 4.50$. We tried to fit the g' formulas keeping the three "intrinsic" principal g values as close to the free-ion g value of 2.0023 as possible, while at the same time requiring C_1 and C_2 to be real numbers. One such fit is $g_z = 2.10$, $g_x = 2.82$, $g_y = 2.52$, $C_1 = 0.0598$, and $C_2 = 0.9983$. We were not able to find a unique set of intrinsic g values, all as close to 2.0023 as possible. Bringing one of the g values close to 2.0023 would make the other two

---

[47] F. Euler and J. A. Bruce, Acta Cryst. **19**, 971 (1965).

[48] N. Pelletier-Allard, Compt. Rend. **260**, 2170 (1965).

[49] R. Pappalardo, D. L. Wood, and R. C. Linares, Jr., J. Chem. Phys. **35**, 1460 (1961).

g values deviate significantly from 2.0023. However, regardless of which set of optimized g values was used, the coefficient C_1 was always very small compared to coefficient C_2, i.e., C_2 was very close to unity. This means that the ground doublet is predominantly an $M_s=\pm\frac{1}{2}$ state with just a small mixing from the $M_s=\pm\frac{3}{2}$ state, a necessary result of the effect of an E term in the Hamiltonian.

The three intrinsic principal g values deviate significantly from the free-electron value. We expect some orbital angular momentum to be introduced into the ground state $^4A_2$ by spin-orbit coupling to the close-lying excited state $^4T_2$. This results in the g value[50] $g=2.0023-8\lambda'/(10\ Dq)$. Here 10 Dq is the separation between the ground state $^4A_2$ and the first excited state and λ' is the effective spin-orbit coupling constant of the Co^{2+} ion in the complex. The value of λ' will be equal to or (because of covalency) less than the spin-orbit coupling constant λ for the free ion. This value of λ is $-180\ cm^{-1}$. If we assume λ' to be about $-150\ cm^{-1}$ and 10 Dq to be about 4000 cm^{-1}, we obtain a g of 2.3. As discussed earlier, the value of 10 Dq found from optical spectral studies of Co-doped $PbMoO_4$ and $PbWO_4$ was about 4500 cm^{-1}, so this argument is not unreasonable. We will not attempt a detailed explanation of the g-tensor anisotropy. Possibly anisotropic spin-orbit interaction[51] would make a contribution.

D. Spin-Lattice Relaxation

In Figs. 3 and 4, the spin-lattice relaxation rate as a function of temperature was plotted on semilog and log-log plots, respectively. It is clear that the experimental data could be fit by two segments of straight lines in both the semilog and the log-log plots. From the semilog plot, the relaxation rate between 10 and 20°K could be assigned to an Orbach-type process of the form $T_1^{-1}\sim e^{-\Delta/kT}$, where Δ is the separation of the ground Kramers states from the nearest excited level. Δ is found to be $83\pm7\ cm^{-1}$ or, in temperature units, 120 ± 10°K. Orbach processes can occur when an excited energy level lies within the phonon spectrum. Recently, the Deybe temperature Θ_D was reported to be 250°K for $CaWO_4$ and 220°K for $PbMoO_4$.[52] These are representative Debye temperatures. We expect a similar value for $PbWO_4$. Since $\Theta_D>\Delta$, an Orbach relaxation mechanism is quite reasonable.

On the log-log scale plot, this part of the data between 10 and 20°K also appears to be a straight line. It could roughly be described by the relation $T_1^{-1}\sim T^9$, i.e., a Raman process. However, it is unlikely that this will be the case here.[53] The $T_1^{-1}\sim T^9$ Raman-process derivation assumes that the excited-state energy value Δ obeys the relation $\Delta\gg\hbar\omega_\varphi$, where $\hbar\omega_\varphi$ is the phonon energy.[54] In the present case, $\Delta(\sim120°K)$ is about half the Θ_D which we have assigned to $PbWO_4$. However, the phonon spectral density increases very rapidly as $\hbar\omega_\varphi$ approaches Θ_D. Hence, although Δ is about one-half of Θ_D, it is not unreasonable that *most* of the phonons have energies *greater* than Δ.

Another type of process could also contribute in this 10–20°K region: relaxation by "local modes."[53,55] If the normal modes of the crystal lattice are perturbed at a defect (i.e., paramagnetic ion) site, the local modes of vibration at such a site could contribute to the spin-lattice relaxation. A necessary condition for the existence of a local mode is a disparity between the mass of the substituent ion and the original site occupant. This certainly is marked when Co substitutes for W (or Pb as well). Such processes have been considered by Feldman, Murphy, Castle[55] and by Klemens.[56] The temperature dependence of the relaxation rate was found to be $T_1^{-1}\sim e^{-\omega_L/kT}$, where ω_L is the frequency of the local mode. From the temperature dependence alone, it cannot be distinguished from the Orbach process.

At low temperatures (4–10°K), the experimental points on the log-log scale plot (Fig. 4) could roughly be described by a straight line with a slope of 4.8 ± 0.3. A special Raman-process result, $T_1^{-1}\propto T^5$, valid when $\Delta\ll\hbar\omega_\varphi$, would explain the relaxation mechanism here.[53,54] Since we presume that most of the phonons possess energy close to the Debye temperature limit we believe that this T^5 analysis applies. A very rough order-of-magnitude argument[54] for the dominance of the T^5 term in the Raman process gives the criterion $\lambda(\lambda/\Delta)\gg kT$. For $\lambda=-150\ cm^{-1}$, $\Delta=83\ cm^{-1}$, $\lambda(\lambda/\Delta)$ turns out to be 271 cm^{-1}. This criterion in our case is easily satisfied.

Although the numerical value of $\Delta(83\ cm^{-1})$ which represents the separation between the ground doublet and the first-excited doublet is unusually large, we will use it to estimate the values of D and E in the spin Hamiltonian. The separation Δ corresponds to $2(D^2+3E^2)^{1/2}$. From the C_1 and C_2 values cited, we find that $D=41.37\ cm^{-1}$ and $E=2.87\ cm^{-1}$. The value of D is large compared to those reported for Co^{2+} in crystals of tetrahedral crystal field symmetry.[16,17,21] On the other hand, our case may not be that typical. EPR spectra of the Co-doped garnets do not seem to be available. It will be recollected that the hfs found in our Co-doped $PbWO_4$ sample was unusually large. Obviously, further work is needed to clarify these points.

V. CONCLUSION

We believe that Co enters the $PbWO_4$ lattice in a 2+ state and probably substitutes at a W site. The ground

---

[50] C. J. Ballhausen, *Introduction to Ligand Field Theory* (McGraw-Hill Book Co., New York, 1962), p. 129.

[51] H. Kamimura, Phys. Rev. **128**, 1677 (1962).

[52] A. A. Antipin, A. N. Katyshev, I. N. Kurkin, and L. Ya. Shekun, Fiz. Tverd. Tela **10**, 1433 (1968) [English transl.: Soviet Phys.—Solid State **10**, 1136 (1968)].

[53] J. Murphy (private communication).

[54] R. Orbach and M. Blume, Phys. Rev. Letters **8**, 478 (1962).

[55] D. W. Feldman, J. G. Castle, Jr., and J. Murphy, Phys. Rev. **138**, A1208 (1965).

[56] P. G. Klemens, Phys. Rev. **138**, A1217 (1965).

state would then be ${}^4A_2$. Since the observed EPR spectrum was characterized by an effective spin of $\frac{1}{2}$ we conclude that the D term in the $S=\frac{3}{2}$ spin Hamiltonian is very large. An E term is also required in view of the g-tensor anisotropy. The orientation of the g-tensor principal axes does not bear any simple geometrical relation to the crystal structure. The hfs is nicely resolved and well separated. Such unusually large hyperfine effects do not occur in other examples of Co^{2+} in tetrahedral (four-coordination and eight-coordination) environments. The EPR spectrum disappears above 20°K due to the onset of rapid spin-lattice relaxation. We suggest that an Orbach-type relaxation process dominates between 10 and 20°K and that the interval 4–10°K is dominated by a T^5 Raman relaxation mechanism. Below 4°K, the resonances saturated easily and "passage effects" were present. No relaxation data were taken in this region. From the temperature trend of the relaxation rate, we estimate that the separation between the ground Kramers doublet and the nearest excited states is several tens of wave numbers. Further optical, microwave, and theoretical investigations should be pursued in this system to obtain a clearer understanding of the reported phenomena.

ACKNOWLEDGMENTS

We wish to express our gratitude to Dr. Joseph Murphy for helpful discussions and suggestions and to Dr. K. K. Sharma for growing the crystal specimens. Thanks are also extended to Dr. J. A. Rayne and to George Sauer, Heinz Lefke, and Gilbert Arnold for their cooperation and technical assistance.

PHYSICAL REVIEW VOLUME 187, NUMBER 2 10 NOVEMBER 1969

Long-Range Order in One-Dimensional Ising Systems

D. J. THOULESS*

Institute for Theoretical Physics, State University of New York, Stony Brook, New York 11790

(Received 17 June 1969)

The argument of Landau and Lifshitz for the absence of long-range order in one-dimensional systems is used to show that order is absent if the interaction energy falls off faster than n^{-2}. When the interaction falls off as n^{-2}, the order cannot go continuously to zero.

THERE is a well-known argument by Landau and Lifshitz[1] which shows that long-range order is not possible in a one-dimensional system with short-range forces. This argument is worth examining closely, because it does divide those versions of the Ising model that are known not to have a phase transition, by the work of Ruelle,[2] from those which are known to possess long-range order at low temperatures, by the work of Dyson.[3] The argument gives particularly interesting results when the interaction between spins m and n is proportional to $(m-n)^{-2}$, for which there is as yet no proof of the presence or absence of long-range order. This form of the Ising model has recently been shown by Anderson and Yuval[4] and by Hamann[5] to be relevant to the theory of the Kondo effect in metals.

For the Ising model, the argument of Landau and Lifshitz can be put in the following terms. We have a line of N spins, with an interaction energy

$$-\sum_{m=2}^{N}\sum_{n=1}^{m-1} J(m-n)S_mS_n\,, \tag{1}$$

where S_n is ± 1. Suppose we have an equilibrium magnetization μN, where μ is between zero and unity. Consider a configuration with this magnetization: We can construct a new configuration with magnetization approximately $\mu(N-2L)$ by reversing the direction of the first L spins. The energy change is

$$\Delta E=2\sum_{m=L+1}^{N}\sum_{n=1}^{L} J(m-n)S_mS_n\,, \tag{2}$$

but there are N possible choices of L, so the entropy change is of the order of

$$\Delta S=\kappa\ln N\,. \tag{3}$$

For a short-range force, the sum on the right-hand side of Eq. (2) is independent of N, and, for sufficiently large N, $\Delta E-T\Delta S$ is always negative, so that the ordered state cannot be the equilibrium state. If we consider interactions $J(n)$ that decrease monotonically as n goes to infinity, it is clear that no interaction

---

* On leave of absence from the University of Birmingham, Birmingham, England.

[1] L. D. Landau and E. M. Lifshitz, *Statistical Physics* (Pergamon Press, Ltd., London, 1958), p. 482.

[2] D. Ruelle, Commun. Math. Phys. **9**, 267 (1968).

[3] F. J. Dyson, Commun. Math. Phys. **12**, 91 (1969).

[4] P. W. Anderson and G. Yuval, Rev. Phys. Letters **23**, 89 (1969).

[5] D. R. Hamann, Phys. Rev. Letters **23**, 95 (1969).